

# Development of a High-Frequency Emissive Probe System for Plasma Potential Measurements in a Hall Thruster

Stéphane Mazouffre, Aude Pétin, Pavel Kudrna, and Milan Tichý

**Abstract**—A heated emissive probe is a smart diagnostic tool for acquisition of the plasma potential in the discharge and in the plume of a Hall thruster. However, measurements of high-frequency oscillations of the potential require a specific electrical circuit with a low  $RC$  time constant. We developed and tested an emissive probe system with a cutoff frequency of 1 MHz. Details about the low-pass filter design as well as first experimental outcomes obtained in the plume of a 200 W permanent magnet Hall thruster are given in this paper.

**Index Terms**—Discharge oscillation, emissive probe, Hall thruster (HT).

## I. INTRODUCTION

A HALL thruster (HT) is an advanced electric propulsion device for satellites and spacecrafts that involves a cross-field electric discharge to ionize and accelerate a propellant gas. The high specific impulse of a HT compared with a chemical engine makes this technology attractive for the maneuvers that require a large velocity increment. In addition, a HT is not current-limited contrary to a gridded ion engine, which allows for a large thrust-to-power ratio. HTs are currently employed for geosynchronous satellite orbit correction and station keeping and such devices will shortly be used for orbit topping and orbit transfer maneuvers and for end-of-life deorbiting. Besides, the success of the SMART-1 Moon flyby solar-powered mission has demonstrated that HTs are good candidates for interplanetary journeys.

A HT is a magnetized low-pressure dc discharge produced between an external cathode and an anode [1]–[3]. The anode, which often serves as gas injector, is located at the upstream end of a coaxial annular dielectric channel that confines the discharge. Xenon is employed as a propellant gas owing to its large atomic mass and low ionization energy. A set of solenoids or permanent magnets generates a radial magnetic field, which is maximum at the channel exhaust. The magnetic field should be strong enough to confine the electrons,

but simultaneously weak enough not to affect ion trajectories. The electric potential drop is mostly concentrated in the final section of the channel owing to the high electron resistivity. The corresponding axial electric field drives an azimuthal electron drift—the Hall current—which is responsible for the efficient ionization of the gas. The electric field also accelerates ions out of the channel, which generates thrust. The beam of positive ions is neutralized by a fraction of electrons emitted by the cathode.

The magnetized plasma of a HT displays numerous types of oscillations, which encompass many kind of physical phenomena each of them with its own length and time scale [4], [5]. Plasma oscillations, of which the spectrum stretches from the kilohertz to the gigahertz frequency domain, play a major role in ionization, particle diffusion, acceleration, and beam characteristics. Time-resolved measurements of plasma parameters are therefore necessary to capture the physical mechanisms that govern the properties and the performance of HTs. Experimental data about the discharge dynamics is also critical for validation of models and the corresponding computer simulations. The plasma potential  $V_p$  is certainly one of the relevant physical quantities to be studied.  $V_p$  can readily be measured by means of a hot emissive probe [6]–[8]. Such an electrical diagnostic tool has been used in recent years to measure the time-averaged and time-dependent plasma potential in the discharge and in the plume of various HTs [9]–[14].

Time-resolved measurements were dedicated to the examination of longitudinal plasma oscillations in the 10–30-kHz band, since they always dominate the power spectrum of a HT, see, for example, [13], [14]. These breathing oscillations originate in a prey–predator-type ionization cycle inside the thruster channel [5], [15]. The electrical circuit linked to an emissive probe does not require an original design to cover the breathing oscillation frequency range. Other types of plasma oscillations are nevertheless of great interest for the physics at play. For instance, the so-called ion transit-time (ITT) instabilities, above 100 kHz, are believed to participate effectively in anomalous electron transport through the magnetic field [16], [17]. However, for frequencies above a few tens of kilohertz, the probe circuit must be carefully built to especially minimize capacitive effects that reduce the cutoff frequency. Another possible approach rests on utilization of an indirectly heated emissive probe [18], [19]. A probe heated by a focused infrared laser beam has a short response time due to the lack of an electrical circuit for heating. However, such a technique is relatively cumbersome. In addition, measurements are difficult

Manuscript received December 16, 2013; revised February 19, 2014; accepted March 20, 2014. Date of publication June 17, 2014; date of current version January 6, 2015. The work of A. Pétin was supported by the French Ministry of Sciences through a Ph.D. Grant.

S. Mazouffre and A. Pétin are with the Centre National de la Recherche Scientifique, ICARE Laboratory, Orléans 45071, France (e-mail: stephane.mazouffre@cnsr-orleans.fr; aude.petin@cnsr-orleans.fr).

P. Kudrna and M. Tichý are with the Faculty of Mathematics and Physics, Charles University, Prague 18000, Czech Republic (e-mail: pavel.kudrna@mff.cuni.cz; milan.tichy@mff.cuni.cz).

Color versions of one or more of the figures in this paper are available online at <http://ieeexplore.ieee.org>.

Digital Object Identifier 10.1109/TPS.2014.2316322

inside the cavity of a HT where the probe must be rapidly moved to minimize disturbances.

In this contribution, we report on the development of a heated emissive probe system with a cutoff frequency around 1 MHz. Several electrical circuits were constructed with different architectures and components. The frequency response of each circuit was measured up to a few megahertz to determine the transmission bands as well as the cutoff frequency. Experiments were performed in the near-field plume of a low-power HT with an optimized low-pass filter. The power spectrum density of the plasma potential time series clearly reveals strong oscillations in the 100–1000-kHz range.

## II. HT AND TEST BENCH

Experiments discussed in this paper were performed with the PPI thruster, a 200 W-class HT which is able to deliver a thrust of 10 mN when operated at 250 V and 1.0 mg/s xenon mass flow rate [20]. This thruster exhibits four interesting features that makes it highly versatile.

- 1) The magnetic field is generated by way of small SmCo magnets brought together inside rings located on either side of the channel walls. A soft iron magnetic circuit with a back gap permits to drive the magnetic flux for obtaining the desired topology. No magnetic screen is used.
- 2) The propellant gas is injected homogeneously inside the channel using a porous ceramic instead of a classical metal hollow gas injector. A stainless-steel ring placed at the back of the channel serves as anode.
- 3) A central copper heat drain is employed to evacuate heat toward a radiator placed behind the thruster.
- 4) The width of the channel can easily be modified keeping the mean diameter unchanged by means of various sets of ceramic rings.

In this paper, the channel walls were made of BN-SiO<sub>2</sub>. The channel was in 2S<sub>0</sub> geometrical configuration that means the width-to-mean diameter ratio was twice the standard one [3], [20], which is defined as the one of the well-known Russian SPT100 thruster. A heated hollow cathode with a LaB<sub>6</sub> insert was used with a mass flow rate of 0.2 mg/s. The applied voltage was 200 V and the anode xenon gas mass flow rate was 1 mg/s. The associated discharge current was 0.94 A.

The PPI thruster was operated in the NExET test bench. The stainless-steel vacuum chamber is 1.8 m long and 0.8 m in diameter. It is equipped with a multistage pumping system that is composed of a large dry pump (400 m<sup>3</sup>/h), a 200 l/s turbomolecular pump to evacuate light gases and a cryogenic pump with a typical surface temperature of 35 K (8000 l/s) to get rid of working gases such as xenon and krypton. A background pressure of  $5 \times 10^{-5}$  mbar-Xe is achieved with a xenon mass flow rate of 1.0 mg/s and an input power of 250 W. The back part of the chamber is water cooled and protected with graphite tiles to absorb a part of the ion beam energy, and thus to reduce the thermal load onto the cryosurface. The chamber is equipped with different observation windows, diagnostic ports as well as electrical and gas feed-throughs. The interior of the test bench is easy to access using a large front door.

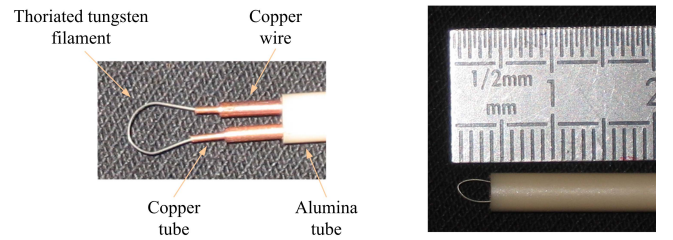


Fig. 1. Emissive probe design and typical sizes.

## III. HIGH-FREQUENCY PROBE SYSTEM

### A. Emissive Probe

The principle of a hot emissive probe is relatively straightforward [6]. The basic idea is to suppress the term connected with the electron temperature  $T_e$  in the formula of the probe floating potential  $V_f$  by introducing an electron emission current  $I_{ee}$ . Assuming Maxwellian electrons and cold ions, that is,  $T_e \gg T_i$ , and in the case of a low emission current, the floating potential then reads

$$V_f = V_p - T_e \ln \left( \frac{I_{s,e}}{I_{s,i} + I_{ee}} \right) \quad (1)$$

wherein  $I_{s,e}$  and  $I_{s,i}$  are the electron and ion saturation currents, respectively. A detailed description of the emissive probe theory and functioning can be found in, for example, [6], [7]. When the filament of a floating probe is sufficiently heated with a dc power supply it enters the regime of electron emission. When  $I_{e,e} \approx I_{s,e} \gg I_{s,i}$ , the floating potential approaches the plasma potential as shown by 1. In the ideal case, the electron current is completely compensated by the emission current from the probe; therefore, no net current flows through the probe and there is no sheath around the probe. However, electrons emitted by the probe are usually colder than the electrons in the plasma. The space charge of the cold electrons limits the emission and a sheath remains around the hot filament [22]. Thus, the measured probe potential is not exactly equal to the plasma potential. If the temperature of the electrons in the plasma is large compared with the temperature of the emitted electrons, which is the case here, the plasma potential is underestimated. The measurement accuracy is typically in the order of the plasma electron temperature.

The emitting part of our probe consists of a  $\approx 6$  mm in length and 0.15 mm in diameter loop of a thoriated tungsten wire mechanically connected to two different copper wires to warrant a high thermal conductivity. The assembly is then inserted into two parallel holes of a 100 mm long and 4 mm in diameter alumina tube. Fig. 1 shows the probe design and sizes [21]. The filament length defines the spatial resolution; it must therefore be small to correctly determine steep potential gradients. A typical emissive probe-heating current-voltage characteristic curve is displayed in Fig. 2. The profile was recorded in the PPI thruster plume near-field along the channel axis. The position  $x = 0$  mm refers to the channel exit plane. When the emission current sufficiently compensates the incoming electron flux, the probe potential jumps to a value close to the local  $V_p$ . Here, the plasma potential is

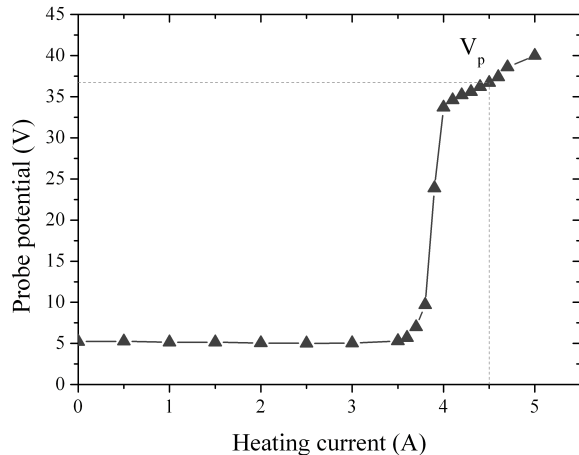


Fig. 2. Development of the probe potential with the heating current. The curve was obtained in the PPI plume nearfield along the channel axis ( $x = 6$  mm). The selected plasma potential  $V_p$  is indicated.

assumed to correspond to a 4.5 A heating current, a value slightly above the knee abscissa. Notice a too high heating current strongly reduces the probe lifetime. Because of the large heating current, the potential drop along the hot probe filament cannot be neglected. A voltage divider bridge must therefore be used in between the probe and the floating power supply ( $R_b = 470 \Omega$ ) to warrant a potential measurement at the probe tip.

### B. Electrical Circuit

An emissive probe used with the floating point method has the advantage of allowing a direct measurement of the time-varying plasma potential. Contrary to a Langmuir probe, no sweep of the probe voltage is required, as previously explained. However, an emissive probe immersed in a plasma represents a resistance ( $R$ ). In addition, the power supply of the heating circuit can be seen as a capacitance to ground ( $C$ ). At first approximation, the probe-circuit assembly therefore forms a  $RC$  circuit, which acts as a filter with a cutoff frequency  $f_{\text{cut}} = 1/2\pi RC$ . The resistance of the hot emissive probe plunged in a HT plasma has been assessed from its  $I-V$  characteristics. The value depends upon the local plasma properties, nonetheless  $R$  is typically around 1 k $\Omega$ . When the probe circuit, that means the dc power supply for heating together with the resistor bridge, is directly connected to the ground, the cutoff frequency is  $\approx 10$  kHz. The capacitance  $C$  is therefore close to 15 nF. This value includes the probe wires and the electrical lines, however, the largest capacitance source is the power supply used for heating. To observe high-frequency plasma oscillations either  $C$  or  $R$  must be decreased. A variety of electrical assemblies can of course be thought of. Only a few examples of possible approaches are given here.

- 1) The equivalent capacitance of the power supply  $C$  can be strongly reduced by isolating the latter from ground through an isolation transformer or an uninterruptible power supply (UPS) that is solely powered by batteries.
- 2) A voltage follower, also termed buffer amplifier, has a high input impedance and a low output impedance, giving effective isolation of the output from the

signal source. When it is inserted into the probe signal path, it decreases the equivalent resistance of the emissive probe.

- 3) The influence of the capacitance  $C$  can be substantially reduced by inserting a passive element with a very low dc resistance and a high ac impedance, that is, an inductor. The emissive probe can then be dc heated and, simultaneously, ac decoupled from the power supply. Because of the ac decoupling, the capacitance  $C$  plays only a minor role and the frequency bandwidth broadens. A set of special choke coils was used for that purpose. A choke here consists of two coils of insulated wire wound in opposite direction on a ring-shape magnetic core. When the current flows through the two coil windings, the magnetic field cancels out and the coils keep a high inductance, typically 2 mH. Such coils have a higher inductance than classic coils. To increase further the total inductance, five chokes were mounted in series. At high frequency, the capacitance can be neglected compared with the coil inductance. At low frequency, the resistance of the coil is nearly zero so the cutoff frequency does not change.

Fig. 3 shows drawings of several electrical circuits built to decrease the  $RC$  time constant of the emissive probe system. The two resistors  $R_b = 470 \Omega$  are the voltage divider bridge resistors, see Section III-A. The hot emissive probe in contact with a HT plasma is here simulated by a 1 k $\Omega$  resistor. The main characteristics of each circuit is the transfer function, or gain. The gain can be determined using a function generator which generates a sine wave with a tunable frequency. The gain  $G$  at a given frequency is then the ratio of the output signal to the input sine wave. A more direct way consists in using a network analyzer. The first method has been used in this paper. The voltage gain in dB unit is plotted as a function of the frequency in Fig. 4 for circuits described in Fig. 3. The gain  $G$  is here defined from the input and output power quantities

$$G = 10 \log \frac{V_{\text{out}}^2}{V_{\text{in}}^2} = 20 \log \frac{V_{\text{out}}}{V_{\text{in}}} \quad (2)$$

where  $V$  is the signal amplitude. Many other circuit architectures have been tested in this paper. The corresponding Bode plots can be found in [23]. For our purpose, three properties are important. The gain must be close to 0 dB over a broad frequency range. Sharp resonances, for example, because of parasitic capacitances, must be avoided.  $f_{\text{cut}}$  must be  $\approx 1$  MHz or higher.

Several conclusions can be drawn from Figs. 3 and 4. The most simple circuit, termed iso, just uses an isolation transformer to transfer the electrical power. That reduces the capacitance  $C$  down to the capacitance between the primary and secondary winding of the transformer, that means around 220 pF. The frequency range that is properly covered is around 600 kHz. The observed dips in the gain curve, see Fig. 4, originate most probably in natural resonances of the primary or secondary windings (wide dip at low frequency) and between the capacitance and the mutual inductance of the coils (dip at higher frequency). Combination of the isolation

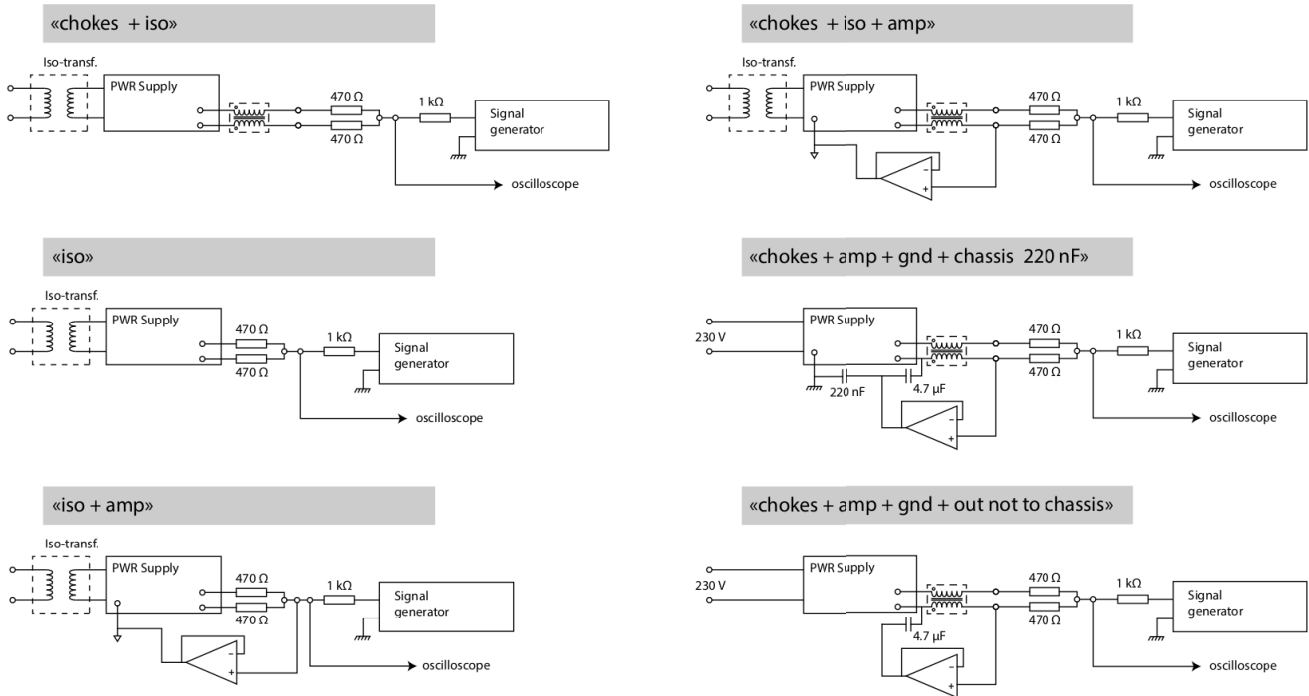


Fig. 3. Drawing of various electrical circuits used to decrease the  $RC$  time constant of the emissive probe system iso: isolation transformer. Amp: amplifier (voltage follower). Gnd: ground. Out: output of the amplifier. Chassis: chassis of the DC power supply.

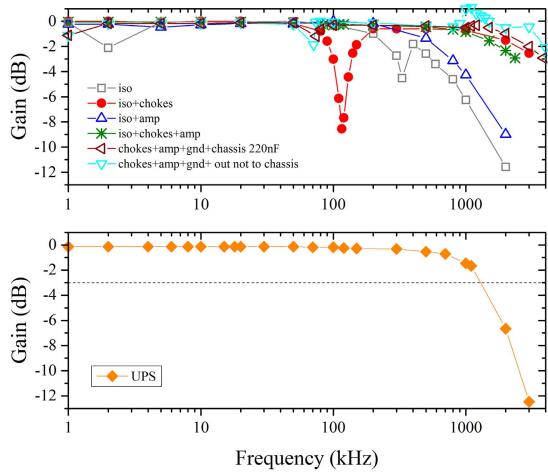


Fig. 4. Gain versus frequency for several emissive probe electrical circuits. The recommended circuit is the one using an UPS.

transformer with the chokes, chokes + iso circuit, increases the frequency bandwidth up to  $\approx 3$  MHz. Nevertheless, a strong dip in the gain curve appears around 100 kHz. It is likely to correspond to the natural resonance of the chokes. Adding a voltage follower to this circuit, chokes + iso + amp circuit, attenuates the dip while keeping the bandwidth rather high. Similarly, the combination of the isolation transformer with the voltage follower, iso + amp circuit, suppresses the dips, but the bandwidth stays below 1 MHz. The last two circuits in Fig. 3 do not involve an isolation transformer. They were tested to verify that a voltage follower is able to attenuate not only the small capacitance of the isolation transformer but also the rather large capacitance of the power supply. Since the body of the power supply is grounded here, the voltage follower drives

directly the power supply output terminals via a sufficiently high capacitor (several  $\mu\text{F}$ ). The two combinations, chokes + iso + gnd + chassis 220 nF and chokes + iso + gnd + out not to chassis circuits, did not bring any substantial improvements compared with, for example, the iso + chokes + amp circuit.

In conclusion, a circuit that solely comprises an isolation transformer or an isolation transformer connected with chokes cannot be employed. In a similar manner, the two circuits based on choke coils with a voltage follower (amplifier) are not suitable. The circuit composed of an amplifier mounted with a choke set and using a transformer to isolate the dc power supply is the most efficient in terms of frequency bandwidth. The cutoff frequency, defined as the  $-3$  dB point, which corresponds to a change in power by a factor of two, is 2.5 MHz, and in addition there is no dip. Another interesting circuit is similar to the previous one but without the choke coils. In that case  $f_{\text{cut}}$  is 0.9 MHz. The most interesting circuit is nevertheless the one for which the power supply is simply isolated from the ground with an UPS solely powered by a set of batteries. It is the simplest system to operate and the most reliable since the amount of components is limited. Besides its cutoff frequency is 1.3 MHz, in agreement with the requirements.

#### IV. PRELIMINARY MEASUREMENTS

##### A. Time-Averaged Plasma Potential

The emissive probe system isolated with a UPS was first used to acquire the time-averaged plasma potential behind the channel exit plane of the PPI HT. A schematic of the experimental arrangement is shown in Fig. 5 along with the coordinate system. The probe was placed parallel to the thruster axis to minimize disturbance of the discharge due

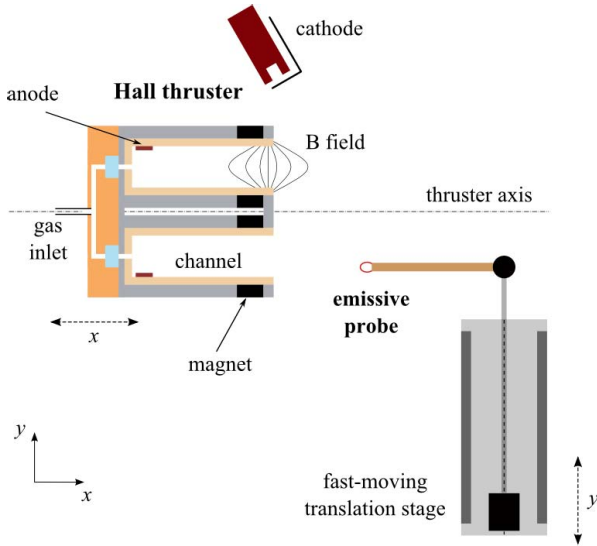


Fig. 5. Schematic of the experimental setup showing the Hall thruster with its cathode and the emissive probe mounted onto the translation stage in parallel configuration (note to scale).

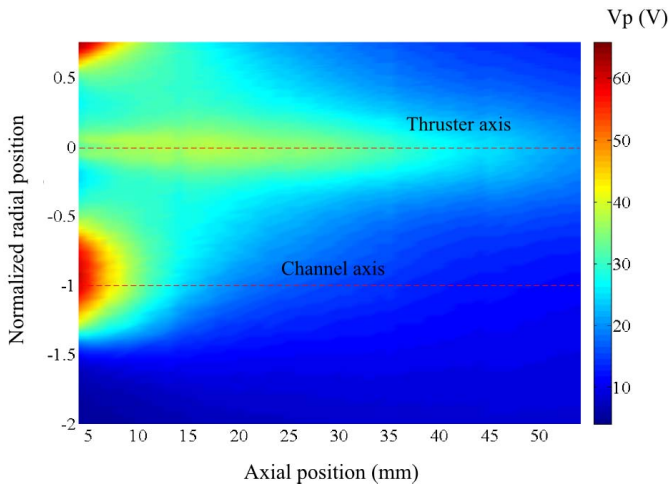


Fig. 6. Contourplot of the plasma potential  $V_p$  behind the channel exhaust of the PPI HT (200 V, 1 mg/s-Xe).

to sputtering of the probe material, especially the ceramic, and secondary electron emission. Details about the impact of probe insertion on the discharge current can be found in [23]. In addition, the residence time of the probe inside the plasma was reduced by means of a fast moving stage to increase the probe lifetime. The displacement system, developed by PILine, is a compact vacuum-compatible ultrasonic linear drive with a maximum speed of 350 mm/s [24]. The probe moved in the radial direction  $y$ . The PPI HT was installed onto a standard translation stage to allow motion in the axial direction  $x$  to fully map  $V_p$ . The contourplot of the plasma potential is shown in Fig. 6. For clarity, the  $y$ -direction has been normalized to the channel mean radius;  $y = 0$  therefore indicates the thruster centerline. The plasma potential is here assumed to be the probe potential heated with a 4.5 A current, see Fig. 2. Above this value, the probe lifetime is strongly reduced. A comparison between Langmuir probe and emissive probe measurements in a HT plume was carried out

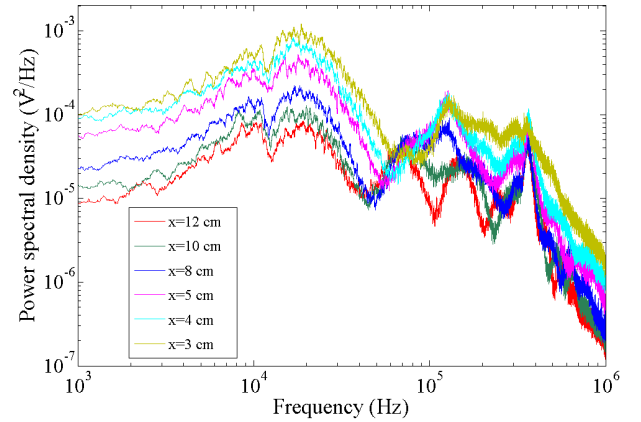


Fig. 7. Power spectral density of the plasma potential for various positions along the channel axis.

in previous works [14]. The plasma potential measured with a similar emissive probe heated with  $\sim 4.5$  A was in good agreement with the potential obtained from the current-voltage trace of a Langmuir probe. However, results have shown that  $V_p$  was slightly overestimated, respectively, underestimated, in regions of low electron temperature, respectively, large electron temperature.

In Fig. 6, the map is symmetrical about the thruster axis as expected.  $V_p$  is maximum on the channel axis. It reaches  $\approx 70$  V at  $x = 4$  mm. The potential is also large on the thruster axis where elementary beams interact. Note that on-axis  $V_p$  goes through a maximum located at  $x = 15$  mm. The electric field reversal in the vicinity of the thruster central part has already been observed by laser spectroscopy [25]. When moving away from the channel exit plane the potential quickly decays due to the expansion of the flowing plasma [26]. Overall, a similar picture has been obtained by Smith and Cappelli in the near field plume of a 200 W-class HT with an emissive probe [12]. The slight differences between the two studies may be due to the geometry and magnetic field topology of the two thrusters.

### B. Time-Varying Plasma Potential

The high-frequency probe system was subsequently used to carry out time-resolved measurements of  $V_p$  along the channel axis of the PPI thruster ( $y = -1$ ). The PPI was fixed and the probe was moved in the  $x$  direction. The voltage divider was connected to a fast oscilloscope in the ac mode for acquisition of the hot probe signal. The time resolution was set to 20 ns. The length of the time series was several tens of breathing oscillation time periods. The power spectral density (PSD) of the time-dependent signal was computed from the Fourier transform of the recorded time-series. Fig. 7 shows the PSD of the signal as a function of the frequency for several positions along the channel axis. The breathing oscillation is the strongest one. The corresponding peak frequency is 19 kHz. A dip appears at 12.4 kHz. It originates most likely in a resonance of the electrical circuit. When  $x = 8$  cm, one can observe a peak at about 72 kHz. Oscillations in this frequency band can be ascribed to azimuthal waves or

ionization instabilities [5]. Oscillations of ITT type are well identified in the 100–600-kHz frequency range. Under our conditions, ion transit time oscillations are relatively strong. Besides, there are two main oscillation groups. One group is characterized by a sharp frequency peak at 370 kHz. The other group exhibits a broad frequency peak around 125 kHz. Moreover, the center frequency seems to depend on the probe position, that is, on the local plasma properties. Our measurements of  $V_p(t)$  indicate that so-called ITT oscillations certainly cover different physical processes. Note that secondary low intensity peaks are visible between 600 kHz and 1 MHz.

## V. CONCLUSION

Several electrical assemblies were developed for measurements of plasma potential oscillations in a HT plasma by using a heated emissive probe system. Depending on the design and components used, the cutoff frequency can be as high as 2.5 MHz, which permits investigation of breathing oscillations, azimuthal waves and ion transit time instabilities. Measurements were performed with the circuit based on an UPS downstream the channel exit plane of a 200 W permanent magnet HT. Despite its simplicity, the system clearly reveals breathing as well as ion transit time oscillations. First measurements indicate a complex physics at play above 100 kHz. Future experiments could aim at better understanding the dynamics of the plasma potential within the ITT mode frequency band. The search for a coupling between the low- and mid-frequency oscillations is important. Besides, the possible role of ITT oscillations in electron transport must be clarified.

## REFERENCES

- [1] V. V. Zhurin, H. R. Kaufman, and R. S. Robinson, "Physics of closed drift thrusters," *Plasma Sources Sci. Technol.*, vol. 8, no. 1, pp. R1–R20, 1999.
- [2] D. M. Goebel and I. Katz, *Fundamentals of Electric Propulsion*. New York, NY, USA: Wiley, 2008.
- [3] K. Dannenmayer and S. Mazouffre, "Elementary scaling relations for Hall effect thrusters," *J. Propul. Power*, vol. 27, no. 1, pp. 236–245, 2011.
- [4] Y. B. Esipchuck, A. I. Morozov, G. N. Tilinin, and A. V. Trofimov, "Plasma oscillations in closed-drift accelerators with an extended acceleration zone," *Soviet Phys. Tech. Phys.*, vol. 18, no. 7, pp. 928–932, 1974.
- [5] E. Y. Choueri, "Plasma oscillations in Hall thrusters," *Phys. Plasmas*, vol. 8, no. 4, pp. 1411–1426, 2001.
- [6] J. P. Sheehan and N. Hershkowitz, "Emissive probes," *Plasma Sources Sci. Technol.*, vol. 20, no. 6, p. 063001, 2011.
- [7] G. D. Hobbs and J. A. Wesson, "Heat flow through a Langmuir sheath in the presence of electron emission," *Plasma Phys.*, vol. 9, no. 1, pp. 85–87, 1967.
- [8] R. F. Kemp and J. M. Sellen, "Plasma potential measurements by electron emissive probes," *Rev. Sci. Instrum.*, vol. 37, no. 4, pp. 455–461, 1966.
- [9] Y. Raitses, D. Staack, M. Keidar, and N. J. Fisch, "Electron-wall interaction in Hall thrusters," *Phys. Plasmas*, vol. 12, no. 5, pp. 057104-1–057104-9, 2005.
- [10] Y. Raitses, D. Staack, A. Smirnov, and N. J. Fisch, "Space charge saturated sheath regime and electron temperature saturation in Hall thrusters," *Phys. Plasmas*, vol. 12, no. 7, p. 073507, 2005.
- [11] J. A. Linnell and A. D. Gallimore, "Internal plasma potential measurements of a Hall thruster using plasma lens focusing," *Phys. Plasmas*, vol. 13, no. 10, p. 103504, 2006.
- [12] A. W. Smith and M. A. Cappelli, "Time and space-correlated plasma potential measurements in the near field of a coaxial Hall plasma discharge," *Phys. Plasmas*, vol. 16, no. 7, pp. 073504-1–073504-11, 2009.
- [13] R. B. Lobbia and A. D. Gallimore, "Method of measuring transient plume properties," in *Proc. 44th AIAA/ASME/SAE/ASEE Joint Propuls. Conf.*, Hartford, CT, USA, Jul. 2008.
- [14] K. Dannenmayer, P. Kudrna, M. Tichý, and S. Mazouffre, "Time-resolved measurement of plasma parameters in the far-field plume of a low-power Hall effect thruster," *Plasma Sources Sci. Technol.*, vol. 21, no. 5, p. 055020, 2012.
- [15] J. P. Boeuf and L. Garrigues, "Low frequency oscillations in a stationary plasma thruster," *J. Appl. Phys.*, vol. 84, no. 7, pp. 3541–3554, 1998.
- [16] S. Barral, K. Makowski, Z. Peradzyński, and M. Dudeck, "Transit time instability in Hall thruster," *Phys. Plasmas*, vol. 12, no. 7, p. 073504, 2005.
- [17] P. Coche and L. Garrigues, "A two-dimensional (azimuthal-axial) particle-in-cell model of a Hall thruster," *Phys. Plasmas*, vol. 21, no. 2, p. 023503, 2014.
- [18] R. Schrittwieser *et al.*, "Laser-heated emissive plasma probe," *Rev. Sci. Instrum.*, vol. 79, no. 8, p. 083508, 2008.
- [19] R. Schrittwieser *et al.*, "Measurements of HF-plasma oscillations by means of a laser-heated emissive probe," *Contrib. Plasma Phys.*, vol. 53, no. 1, pp. 92–95, 2013.
- [20] S. Mazouffre, G. Bourgeois, K. Dannenmayer, and A. Lejeune, "Ionization and acceleration processes in a small, variable channel width, permanent-magnet Hall thruster," *J. Phys. D, Appl. Phys.*, vol. 45, no. 18, p. 185203, 2012.
- [21] K. Dannenmayer, "Scaling laws and electron properties in Hall effect thrusters," Ph.D. dissertation, Univ. Orléans, Orléans, France, 2012.
- [22] S. Takamura, N. Ohno, M. Y. Ye, and T. Kuwabara, *Contrib. Plasma Phys.*, vol. 44, nos. 1–3, p. 126, 2004.
- [23] A. Pétin, S. Mazouffre, K. Dannenmayer, P. Kudrna, and M. Tichý, "Time-averaged and time-varying plasma potential in the near field plume of a Hall thruster," in *Proc. 33rd Int. Electr. Propuls. Conf.*, Washington, DC, USA, 2013, pp. 1–9, no. 2013-214.
- [24] K. Dannenmayer and S. Mazouffre, "Compact high-speed reciprocating probe system for measurements in a Hall thruster discharge and plume," *Rev. Sci. Instrum.*, vol. 83, no. 12, p. 123503, 2012.
- [25] A. Lejeune, G. Bourgeois, and S. Mazouffre, "Kr II and Xe II axial velocity distribution functions in a cross-field ion source," *Phys. Plasmas*, vol. 19, no. 7, p. 073501, 2012.
- [26] K. Dannenmayer and S. Mazouffre, "Electron flow properties in the far-field plume of a Hall thruster," *Plasma Sources Sci. Technol.*, vol. 22, no. 3, pp. 035004-1–035004-4, 2013.

Authors' photographs and biographies not available at the time of publication.